

consider effects of eruption rate and vent geometry during magma withdrawal from crustal reservoirs. □

Received 13 November 1989; accepted 12 April 1990.

- Hildreth, W. *J. geophys. Res.* **86**, 10153–10192 (1981).
- Carrigan, C. R. & Eichelberger, J. C. *Nature* **343**, 248 (1990).
- Spera, F. J. *J. geophys. Res.* **89**, 8222–8236 (1984).
- Spera, F., Yuen, D., Greer, J. & Sewell, G. *Geology* **14**, 723–726 (1986).
- Blake, S. & Ivey, G. N. *J. Volcan. geotherm. Res.* **27**, 153–178 (1986).
- Blake, S. & Ivey, G. N. *J. Volcan. geotherm. Res.* **30**, 201–230 (1986).
- Freundt, A. & Tait, S. *Bull. Volcan.* **48**, 325–339 (1986).
- Sigurdsson, H., Carey, S., Cornell, W. & Pescatore, T. *Nat. geogr. Res.* **1**, 332–387 (1985).
- Carey, S. & Sigurdsson, H. *Bull. geol. Soc. Amer.* **99**, 303–314 (1987).
- Carey, S. & Sparks, R. S. J. *Bull. Volcan.* **48**, 109–125 (1986).
- Wilson, L. & Walker, G. P. L. *Geophys. J. R. astr. Soc.* **63**, 651–679 (1987).
- Cornell, W. *thesis, Univ. Rhode Island* (1987).
- Carey, S. & Sigurdsson, H. *Bull. Volcan.* **51**, 28–40 (1989).
- Druitt, T. & Sparks, R. S. J. *Nature* **310**, 679–681 (1984).

ACKNOWLEDGEMENTS. We thank T. Druitt for his review of the manuscript. This work was supported by the National Science Foundation and the National Geographic Society.

High-field-strength element depletions in arc basalts due to mantle–magma interaction

P. B. Kelemen*, K. T. M. Johnson*, R. J. Kinzler† & A. J. Irving‡

* Department of Geology and Geophysics, Woods Hole Oceanographic Institution, Woods Hole, Massachusetts 02543, USA

† Department of Earth, Atmospheric and Planetary Sciences, Massachusetts Institute of Technology, Cambridge, Massachusetts 02139, USA

‡ Department of Geological Sciences AJ-20, University of Washington, Seattle, Washington 98195, USA

BASALTS, basaltic andesites and andesites in subduction-related magmatic arcs are all depleted in high-field-strength elements (such as Ti, V, Zr, Nb, Hf and Ta) relative to mid-ocean-ridge basalt (MORB). Here we show that these depletions can be produced in liquids by interaction with depleted mantle peridotite, as would occur during the ascent of an arc magma through the mantle lithosphere of the overriding plate. This process involves extensive reaction between liquid, olivine, orthopyroxene and spinel. High-field-strength element depletions are produced because olivine, orthopyroxene and spinel have higher crystal/liquid distribution coefficients for these elements than for other incompatible trace elements. Liquids modified by mantle–magma interaction will also be depleted in heavy rare-earth elements, Cr and Ni, and enriched in light rare-earth and large-ion lithophile elements, relative to MORB. These characteristics are all common in mafic magmas at convergent plate margins^{1–7}.

Our trace-element modelling complements recent experimental and theoretical investigations, which show that reaction between magnesian olivine tholeiite and depleted peridotite can produce the major-element characteristics of calc-alkaline basalt, basaltic andesite and andesite^{8–12}. Calc-alkaline andesites are found almost exclusively in subduction-related magmatic arcs². Effects of interaction between ascending liquid and upper-mantle wall rock will be enhanced where magma ascends slowly through narrow conduits or by grain-boundary infiltration. The absence of high-field-strength element (HFSE) depletions in most MORBs and back-arc basin basalts is therefore ascribed to relatively limited interaction between liquids and mantle peridotite, due to rapid aggregation and ascent of partial melts at divergent-plate margins.

HFSE depletions have been defined in the following two ways. (1) Many primitive magmas in subduction-related magmatic arcs have abundances of HFSE, heavy rare-earth elements (HREEs) and some compatible elements (Cr, Ni) that are lower

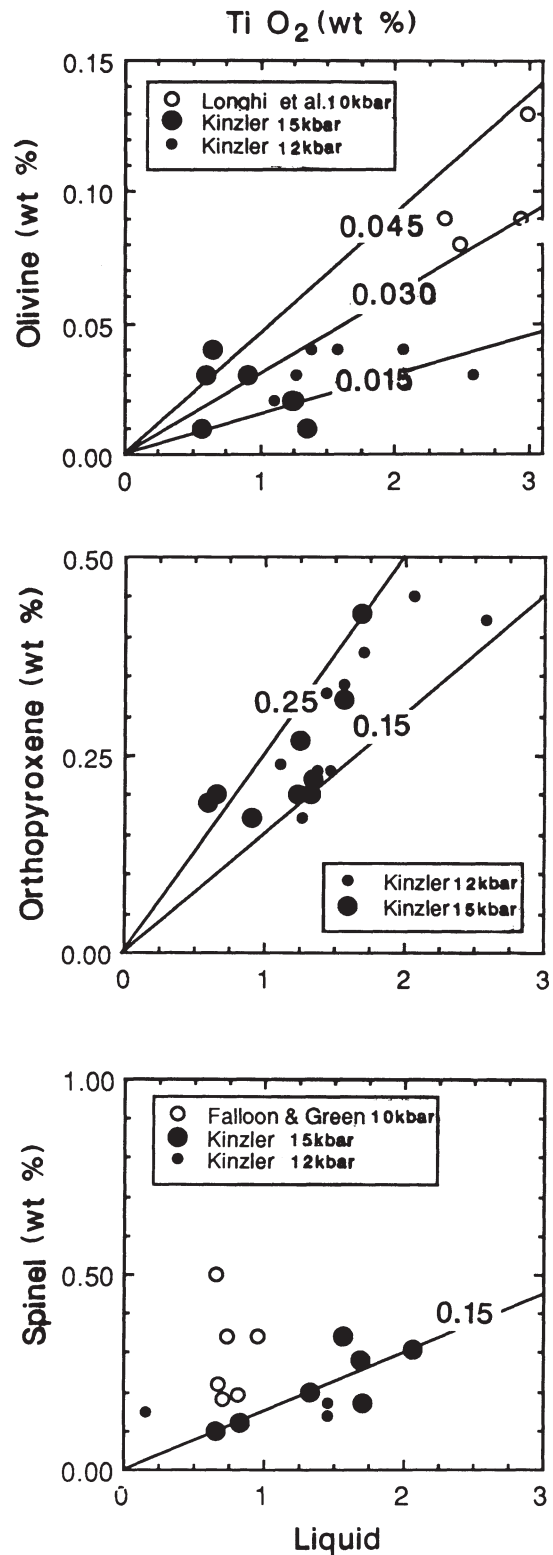


FIG. 1 Electron-microprobe analyses of TiO_2 (weight per cent) in coexisting olivine, orthopyroxene, Cr–Al spinel and liquid (quenched glass) from experiments on magnesian basalt compositions at pressures ≥ 10 kbar. On the basis of these and other data^{22–27} we have adopted values of 0.015 for $D_{\text{liq}}^{\text{ol}}(\text{TiO}_2)$, 0.15 for $D_{\text{liq}}^{\text{opx}}(\text{TiO}_2)$, and 0.15 for $D_{\text{liq}}^{\text{spinel}}(\text{TiO}_2)$ in the upper mantle. Data of Longhi *et al.*²⁴ are for lunar basalts at an oxygen fugacity buffered by Fe–FeO. Data of Falloon and Green³⁷ are for basalt–peridotite mixtures at 10 kbar. Data of Kinzler (this paper and R.J.K. and T. L. Grove, manuscript in preparation) are for MORB + olivine bulk compositions at 12 and 15 kbar. Oxygen fugacity was not buffered in the experiments of ref. 37 and of R.J.K. and T. L. Grove, but all were performed in graphite inner capsules.

than those of primitive MORB. These characteristics have been attributed to the stabilization of a phase with HFSE crystal/liquid distribution coefficients ($D_{\text{liq}}^{\text{xl}} = \text{concentration in crystal}/\text{concentration in liquid}$) > 1 in the arc magma source, to metasomatism of the arc magma source by a fluid or magma depleted in HFSE, to a high degree of partial melting, and/or to early fractionation of magnetite^{1-7,13,14}. In general agreement with our study¹⁵, Meen and Ayers¹⁶ attributed HFSE depletions to reaction with mantle wall rock. (2) HFSE anomalies have been defined as depletions or enrichments of HFSEs relative to the adjacent elements on compatibility diagrams. The order of elements on such diagrams has been determined on the basis of smoothness of the normalized trace-element pattern of MORB (ref. 17 and references cited therein). The Zr anomaly is defined as $2Zr/(Sm + Nd)$, and Ti anomaly as $2Ti/(Eu + Tb)$, using chondrite-normalized concentrations. Where the anomalies are less than unity for HFSEs in a solid or liquid phase, the phase is considered depleted in HFSEs. Depletions defined in this way are common in arc magmas^{4-7,13,14}, and occur in clinopyroxenes from mantle peridotites^{18,19}. Mantle-magma interaction can produce both types of HFSE depletion.

We have used Zr and Ti as analogues for all HFSEs. The crystal/liquid distribution coefficients for other HFSEs in olivine (ol), orthopyroxene (opx) and spinel are virtually unknown. We use generally accepted values of $D_{\text{liq}}^{\text{xl}}$ for rare-earth elements (REEs), Zr and Ti, supplemented by new experimental data for $D_{\text{liq}}^{\text{spinel}}$, $D_{\text{liq}}^{\text{opx}}$ and $D_{\text{liq}}^{\text{ol}}$. There is considerable uncertainty in these

values owing to inhomogeneity of products in experiments, analytical errors arising from low concentrations, and incomplete characterization of variation of $D_{\text{liq}}^{\text{xl}}$ with temperature, pressure and bulk composition. It is especially worrisome that $D_{\text{liq}}^{\text{xl}}$ for REEs, Ti and Zr have rarely been measured in the same experiment. Here we adopt the lowest $D_{\text{liq}}^{\text{xl}}$ for Ti and Zr compatible with experimental data. These minimize fractionation of HFSEs by reaction; larger values would produce larger HFSE depletions. An essential point is the adoption of $D_{\text{liq}}^{\text{ol}}$ for REEs determined by McKay²⁰. Slightly higher values from the algorithm of Colson *et al.*²¹ could be used, but the algorithm does not fit McKay's data for light rare-earth elements (LREEs). We consider much higher values of $D(\text{REE})_{\text{liq}}^{\text{ol}}$ to be incorrect, in agreement with McKay²⁰. Aside from this, the qualitative results of our modelling can be reproduced using virtually any consistent set of $D_{\text{liq}}^{\text{xl}}$ from the literature.

Published $D_{\text{liq}}^{\text{xl}}$ for Zr and Ti in olivine and orthopyroxene²⁰⁻²⁷, and new results presented here (Fig. 1) for Ti in olivine, orthopyroxene and Cr-Al spinel, show that these two HFSEs have $D_{\text{liq}}^{\text{xl}}$ s that are orders of magnitude larger than $D_{\text{liq}}^{\text{xl}}$ for REEs in these phases (Table 1 and references cited therein). Zr and Ti are not strongly fractionated from the REEs in liquids produced by partial melting (Fig. 2a). But during mantle-magma interaction, liquid may react with large masses of olivine, or orthopyroxene and spinel, and these phases will fractionate Zr and Ti relative to REEs (Fig. 2b-d).

We modelled mantle-magma interaction using the equations in refs 8 and 28 for combined assimilation and crystal fractionation. Results are presented in Fig. 2. The reactants used are depleted-mantle lherzolite (Fig. 2 and Table 1), and aggregate liquid from 3% melting of pyrolite²⁹ (Fig. 2). Liquids formed by partial melting of four-phase peridotite will become saturated only in olivine (\pm Cr-rich spinel) on decompression³⁰⁻³². Their reaction with lherzolite will involve incongruent dissolution of pyroxene to produce olivine + spinel + modified liquid. Although decompression alone should increase the mass of liquid in mantle-magma systems, we suggest that this effect may be balanced in natural systems by cooling and chemical effects of wall-rock reaction⁸⁻¹⁰ during ascent. For example, possible increase in magma mass owing to pyroxene dissolution would decrease the water content of initially hydrous liquids, leading to increased crystallization. For these reasons, and for simplicity, we model mantle-magma interaction with constant magma mass (mass assimilated/mass crystallized, $M_a/M_c = 1$).

Three different types of reaction between basaltic magma and lherzolite are illustrated. (1) In Fig. 2a dissolution of pyroxene is small, so phase proportions in the lherzolite remain constant. (2) In Fig. 2b ascending magma dissolves some pyroxene, but not all, leaving a harzburgite residuum. (3) In Fig. 2c all pyroxene in the wall rock dissolves, leaving a dunite residuum. Liquid products of reactions involving extensive pyroxene dissolution will probably be calc-alkaline basalt, basaltic andesite and andesite; derivative liquids of reactions involving minimal pyroxene dissolution will generally be tholeiitic⁸⁻¹⁰. All these reactions produce depletions of Zr and Ti in derivative liquids. Reactions (1) and (2) also lead to depletion of REEs relative to MORB. If liquid mass decreases slightly ($M_a/M_c = 0.9990$), owing to reaction stoichiometry and/or cooling of ascending magma, Cr and Ni are also depleted.

Many of the distinctive trace-element characteristics of primitive arc magmas can be accounted for by reactions in which liquids formed by partial melting of fertile peridotite at depth interact with depleted upper-mantle wall rocks during ascent. During the formation of ocean crust, the uppermost mantle is subjected to the largest degree of melting, with progressively deeper lherzolites undergoing progressively less depletion in basaltic components. We envision an initial state in which such variably depleted mantle becomes part of the overthrust plate in a subduction zone. Melting of a fertile source produces liquids that rise through, and react extensively with, more-depleted

TABLE 1 Phase proportions and distribution coefficients used in modelling

(a) Phase proportions (weight per cent)					
	Pyrolite ²⁹	Melting mode*	Iherzolite (residue of 16.5% melting of pyrolite)	Harzburgite (50% iherzolite 50% dunite)	Dunite
Olivine	55.2	-20	69	83	97
Orthopyroxene	24.7	25	24	12	0
Clinopyroxene	17.8	83	5	2.5	0
Spinel	2.3	2	2	2.5†	3†

(b) Crystal/liquid distribution coefficients at ~10 kbar (by weight)				
	Olivine‡	Orthopyroxene§	Clinopyroxene	Spinel¶
La	0.000007	0.0025	0.04	0.0006
Ce	0.00001	0.005	0.13	0.0006
Nd	0.00007	0.01	0.25	0.0006
Zr	0.007	0.07	0.20	0.07
Sm	0.0007	0.02	0.45	0.0006
Eu	0.00095	0.03	0.50	0.0006
Gd	0.0012	0.04	0.50	0.0006
Ti	0.015	0.15	0.30	0.15
Dy	0.004	0.05	0.51	0.0015
Er	0.009	0.07	0.52	0.003
Yb	0.023	0.11	0.52	0.0045
Cr	2.0	8.0	2.0	200.0
Ni	11.0	3.5	3.0	10.0

* The melting mode was determined by solution of the matrix $X \cdot \text{ol} + X \cdot \text{opx} + X \cdot \text{cpx} + X \cdot \text{spinel} = 100 \cdot \text{liq}$ using data on coexisting liquid and solid phases in spinel lherzolite at 10-20 kbar, adjusted to produce approximately constant modal proportion of spinel during melting.

† The modal proportion of spinel produced by pyroxene dissolution is calculated assuming that virtually all Cr in pyroxene reactants consumed is incorporated in spinel, pyroxenes contain ~1 wt% Cr₂O₃, and the proportion of Cr₂O₃ in spinel is approximately constant at 30 wt%.

‡ REEs, ref. 20; Zr and Ti, refs 23-27, this paper, P.B.K., unpublished ion-probe data, R. J. K. and T. L. Grove, manuscript in preparation; Cr and Ni, ref. 23 and references cited therein.

§ REEs, ref. 35, clinopyroxene partition coefficients; Zr and Ti, ref. 22, this paper, R. J. K. and T. L. Grove, manuscript in preparation; Cr and Ni, ref. 23 and references cited therein.

|| REEs, ref. 36, K. T. M. J. and R. J. K., unpublished ion-probe data; Zr and Ti, ref. 23 and references cited therein, refs 25, 26, 36, K.T.M.J. and R.J.K., unpublished ion-probe data; Cr and Ni, ref. 23 and references cited therein.

¶ REEs, ref. 35, clinopyroxene partition coefficients; Zr, by analogy to clinopyroxene with $2D(\text{Zr}) \geq D(\text{Ti})$; Ti, this paper, R. J. K. and T. L. Grove, manuscript in preparation; Cr and Ni, ref. 23 and references cited therein.

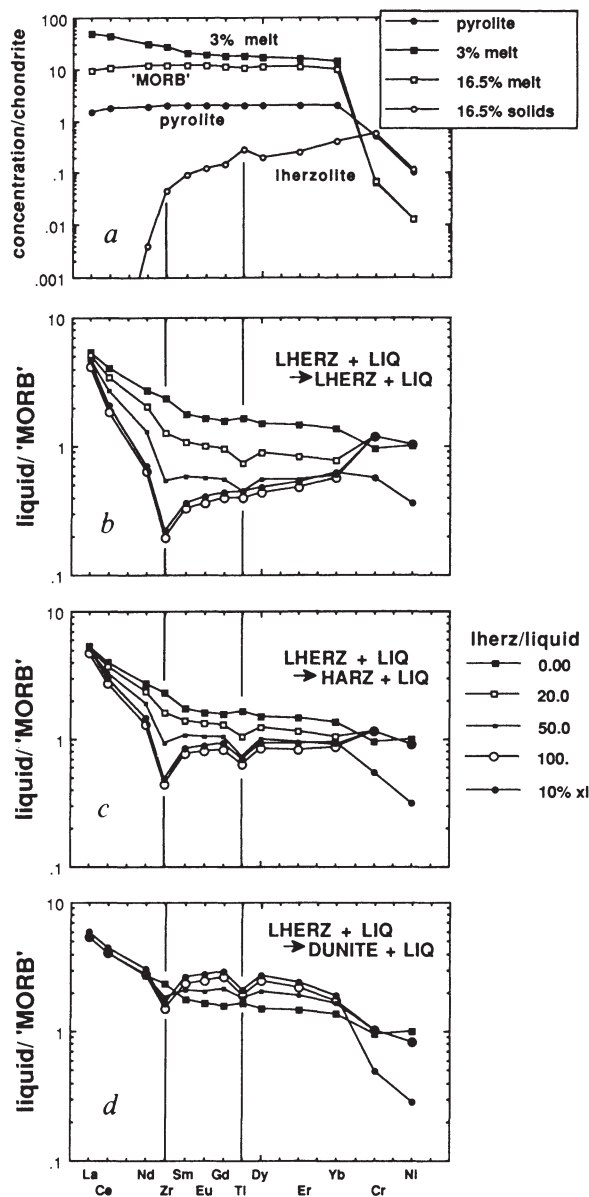


FIG. 2 Results of modelling the reaction between basaltic magma and depleted-mantle lherzolite. Phase assemblages, bulk compositions and D_{liq}^x s given in Table 1. *a*, Initial solid and liquid compositions used in modelling. Initial compositions produced by fractional melting of pyrolite²⁹. Fractional melting does not significantly fractionate HFSEs from REEs in aggregate liquids. This is true for liquids produced by batch melting (not shown) as well. Curve labelled 3% is aggregate liquid from 3% fractional fusion. MORB is putative mid-ocean-ridge-basalt composition, and is the aggregate liquid formed by 16.5% fractional fusion. Lherzolite is the bulk-solid composition after 16.5% fractional fusion, and is similar to abyssal peridotites, which have strongly depleted REE patterns¹⁹. Initial pyrolite composition has REEs from 1.5 (for La) to 2 (for Sm to Yb) times the chondritic abundance, Zr and Ti = 2 × (chondritic), Cr = 0.5 × (chondritic), and Ni = 0.1 × (chondritic)^{38,39}. Order of elements as for compatibility diagrams of ref. 17 and references cited therein. *b*, *c*, *d*, Results of reaction between basalt and depleted lherzolite: Wall-rock reaction in the upper mantle produces HFSE depletion, accompanied by HREE depletion relative to MORB, in derivative liquids. Initial liquid (mass lherz/mass liquid = 0.00) is aggregate melt from 3% fractional melting of pyrolite. Lherzolite reactant is residue of 16.5% fractional melting of pyrolite. Reaction modelled using equations of refs 29 and 8. Key to abbreviations: 'MORB' = aggregate melt produced by 16.5% fractional melting of pyrolite; LHERZ, HARZ, DUNITE denote lherzolite, harzburgite and dunite phase assemblages, respectively; LIQ, liquid; lherz/liquid, mass of lherzolite reactant to mass initial liquid in the system. All calculations for constant magma mass except curves labelled 10% xl. In these, magma mass decreases 10% during reaction, mass lherz reactant to mass liquid = 100, and $M_a/M_c = 0.9990$.

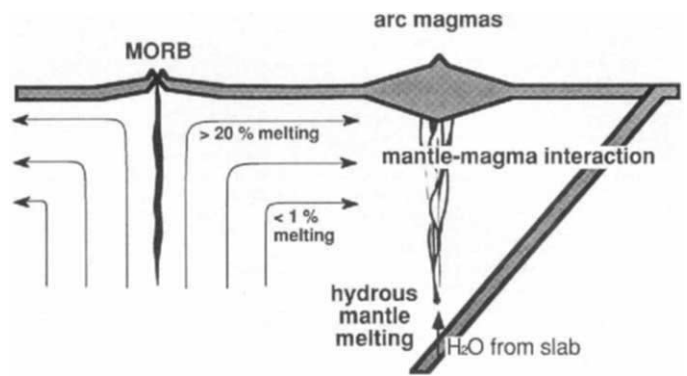


FIG. 3 Schematic illustration of mantle melting processes. At spreading centres, the aggregate melts of large degrees of fractional melting rise to form MORB. In subduction zones, H₂O from the downgoing slab rises into the mantle and causes small degrees of partial melting in fertile mantle at depth. Liquids generated here pass slowly upward through, and interact with, depleted peridotite wall rock.

mantle lithosphere on their way to form new arc crust (Fig. 3). Both liquid and solid products of reaction will develop HFSE and HREE depletion during this process. This hypothesis is consistent with the theory that some calc-alkaline basalts, basaltic andesites and andesites are produced by reaction between ascending tholeiitic magmas and mantle wall rock⁸⁻¹⁰.

We believe that the following results are general: reaction will produce depletions relative to MORB in Zr, Ti and REEs in derivative liquids. Where initial liquids are enriched in REEs and large-ion lithophiles relative to MORB, this enrichment will be retained in derivative liquids. Where magma mass decreases slightly during reaction, concentration of Cr and Ni in derivative liquids will be lower than in primitive MORB. Although reaction will produce large variations in trace-element concentration, Mg/(Mg + Fe) will be high and approximately constant in derivative liquids⁸⁻¹⁰.

Our calculations do not require ascending liquid to reach major-element or trace-element equilibrium with surrounding mantle wall rock. Calculated mass ratios of reactant lherzolite to initial liquid are similar to fluid/rock ratios in metamorphic petrology. They represent the minimum mass of lherzolite necessary to produce a given liquid composition, assuming complete equilibrium between reactants is attained. Our results would be qualitatively unchanged even if some reaction mechanisms, such as dissolution of pyroxenes, were more rapid than others, such as solid diffusion in olivine and spinel. Our results are, however, dependent on the implicit assumption that rates of exchange reactions for Zr and Ti are greater than or equal to rates of exchange reactions for REEs, on the timescale of mantle-magma interaction.

Isotope analyses of many arc magmas indicate the presence of a slab-derived component in their source (refs 1, 2, 33, 34 and references cited therein). But the slab-derived component need not have the trace-element characteristics, such as HFSE depletion, which distinguish arc basalts from MORBs. Although other hypotheses are viable, we believe that the essential contribution of the slab-derived component in arc magmatism is water, which leads to partial melting in the overlying mantle wedge. HFSE depletions arise as partial melts formed in the wedge move slowly up and react with mantle wall rock. □

Received 20 February; accepted 11 April 1990.

- Perfit, M. R., Gust, D. A., Bence, A. E., Arculus, R. J. & Taylor, S. R. *Chem. Geol.* **30**, 227-256 (1980).
- Gill, J. B. *Orogenic Andesites* (Springer, New York, 1981).
- Arculus, R. J. & Johnson, R. W. *Geochem. J.* **15**, 109-133 (1981).
- Pearce, J. A. in *Andesites* (ed. Thorpe, R. S.) 525-598 (Wiley, New York, 1982).
- Hickey, R. L. & Frey, F. A. *Geochim. cosmochim. Acta* **46**, 2099-2115 (1982).
- Dupuy, C. et al. *Earth planet. Sci. Lett.* **60**, 207-225 (1982).
- Hole, M. J., Saunders, A. D., Marriner, G. F. & Tarney, J. *J. geol. Soc. Lond.* **141**, 453-472 (1984).

8. Kelemen, P. B. *J. Geol.* **94**, 829–843 (1986).
9. Kelemen, P. B. *J. Petrol.* **31**, 51–98 (1990).
10. Kelemen, P. B., Joyce, D. M., Webster, J. D. & Holloway, J. R. *J. Petrol.* **31**, 99–134 (1990).
11. Fisk, M. R. *Geophys. Res. Lett.* **13**, 467–470 (1986).
12. Carroll, M. R. & Wyllie, P. J. *J. Petrol.* **30**, 1351–1382 (1989).
13. Arculus, R. J. & Powell, R. *J. geophys. Res.* **91**, 5913–5926 (1986).
14. Ryerson, F. J. & Watson, E. B. *Earth planet. Sci. Lett.* **86**, 225–239 (1987).
15. Kelemen, P. B., Johnson K. T. M. & Kinzler R. J. *Eos* **70**, 1387–1388 (1989).
16. Meen, J. K. & Ayers, J. C. *New Mex. Bur. Min. miner. Resour. Bull.* **131**, 185 (abstr.) (1989).
17. Sun, S. S. & McDonough, W. F. *Spec. Pap. geol. Soc. Am.* **42**, 313–345 (1989).
18. Salters, V. J. & Shimizu, N. *Geochim. cosmochim. Acta* **52**, 2177–2182 (1988).
19. Johnson, K. T. M., Dick, H. J. B. & Shimizu, N. *J. geophys. Res.* **95**, 2661–2678 (1990).
20. McKay G. A. *Geochim. cosmochim. Acta* **50**, 69–79 (1986).
21. Colson, R. O., McKay, G. A. & Taylor, L. A. *Geochim. cosmochim. Acta* **52**, 539–553 (1988).
22. Grove, T. L. & Bence, A. E. *Proc. lunar planet. Sci. Conf.* **7**, 1549–1579 (1976).
23. Irving, A. J. *Geochim. cosmochim. Acta* **42**, 743–770 (1978).
24. Longhi, J., Walker, D. & Hays, J. F. *Geochim. cosmochim. Acta* **42**, 1545–1558 (1978).
25. Fujimaki, H., Tatsumoto, M. & Aoki, K. *Proc. lunar planet. Sci. Conf.* **14**, Part 2 in *J. geophys. Res., Suppl.* **89**, B662–B672 (1984).
26. Dunn, T. *Contrib. Miner. Petrol.* **96**, 476–484 (1987).
27. Ulmer, P. A. *Rep. Director, Geophysical Lab.* 42–47 (Carnegie Inst., Washington DC, 1989).
28. DePaolo, D. J. *Earth planet. Sci. Lett.* **57**, 47–62 (1981).
29. Ringwood, A. E. in *Advances in Earth Science* (ed. Hurley, P. M.) 287–356 (Mass. Inst. Technol. Press, 1966).
30. O'Hara, M. *Scot. J. Geol.* **1**, 19–40 (1965).
31. Stolper, E. *Contrib. Miner. Petrol.* **74**, 13–27 (1980).
32. Elthon, D. & Scarfe, C. M. *Carnegie Inst. Wash. Yb.* **79**, 277–281 (1980).
33. Tera, F. *et al. Geochim. cosmochim. Acta* **50**, 535–550 (1986).
34. Davidson, J. P. *Geochim. cosmochim. Acta* **51**, 2185–2198 (1987).
35. Stosch, H. G. *Geochim. cosmochim. Acta* **46**, 793–811 (1982).
36. Green, T. H. & Pearson, N. J. *Contrib. Miner. Petrol.* **91**, 24–36 (1985).
37. Falloon, T. J. & Green, D. H. *Miner. Petrol.* **37**, 181–219 (1989).
38. Loubet, M., Shimizu, N. & Allegre, C. J. *Contrib. Miner. Petrol.* **53**, 1–12 (1975).
39. Jagoutz, E. *et al. Proc. lunar planet. Sci. Conf.* **10**, 2031–2050 (1979).

ACKNOWLEDGEMENTS. We thank R. Arculus, J. Davidson, H. Dick, F. Frey, J. Gill, V. Salters, N. Shimizu, T. Sisson and B. Wasson for comments on the manuscript. This work was supported in part by the Woods Hole Oceanographic Institution.

Induced vertical migration in copepods as a defence against invertebrate predation

William E. Neill

Ecology Group, Department of Zoology, 6270 University Boulevard, University of British Columbia, Vancouver, BC V6T 2A9, Canada

The adaptive significance of diel vertical migration by planktonic organisms is often explained in terms of daily changes in foraging locations that reduce the risk of depth-stratified predation^{1–3}. The timing, extent and rate of migration are usually presumed to be more or less invariant (closed⁴) behaviours that have evolved under local predation regimes^{5–8}. Observational and experimental evidence, however, indicate that migratory patterns in the presence of predators may be altered substantially by short-term reduction in the availability of food^{9–13}. Behavioural flexibility of food-limited individuals rather than genetic change of populations seems likely¹³. Whether individuals are also sensitive to changes in the risk of predation is unknown, though some field observations are highly suggestive¹⁴. Here I report rapid initiation (<4 h) of vertical migration in previously non-migrating freshwater copepods inside large *in situ* enclosures on exposure to an invertebrate predator. Responses of copepods to water that had previously held captive predators suggests that a chemical cue is involved. These results show that crustacean zooplankton may be capable of flexible, predator-sensitive foraging and suggest a mechanism for rapid changes in migration patterns.

Larval phantom midges *Chaoborus* spp. (Diptera; Chaoboridae) are large, 'nocturnal'¹⁴ vertical migrators (night-time ascent, daytime descent) that eat other freshwater zooplankton. Some prey taxa abandon more productive shallow strata during nocturnal incursions of chaoborids and establish opposing 'reverse' vertical migrations^{15,16} (night-time descent, daytime ascent). I examined a reverse migration by the calanoid copepod *Diatomus kenai* in oligotrophic Gwendoline Lake (49°19' N, 122°34' W, 13 ha, 27 m maximum depth, mean Secchi

depth 8 m) before and after chaoborids were eliminated by escaped juvenile trout (*Salmo clarki*). Predatory mortality of copepods (annually ~20% (refs 16, 17)) became negligible for the next 3 yr (no invertebrate predators of copepods detected in 166 bi-weekly plankton samples and only 9 *D. kenai* in 27,128 diet items from 88 netted and angled trout) as trout focused on abundant alternative prey.

When re-examined 28 months (four copepod generations) after midge extermination, the enhanced population of *D. kenai* had ceased migrations (Fig. 1). All copepods continuously occupied more productive shallow waters previously exploited only during daylight hours. Grazable algal concentrations were 30–50% higher than in pre-fish samples (Fig. 1), presumably as a result of reduced cladoceran grazing under fish predation. Whether migratory behaviour had been lost through natural selection for non-migratory morphs or through phenotypic plasticity of individuals, and whether increased abundance of phytoplankton had any measurable consequences on altered migration were examined in experimental enclosures.

I exposed *D. kenai* from Gwendoline Lake, which had been free of phantom midge predation for four copepod generations, to imported *Chaoborus trivittatus* inside 1.5 m × 15 m deep polyethylene tubes inserted in Gwendoline Lake. Migratory fourth instar midge larvae (2,500 per enclosure, collected in a nearby fishless lake) and Gwendoline Lake zooplankton were stocked at historical pre-fish densities. No fish were stocked in any enclosures. Triplicate 100-litre, depth-stratified pump samples¹⁷ taken at 1.5 m intervals were used to estimate plankton densities and document vertical spatial distributions. Sampling began 4 h after adding crustaceans and chaoborids to enclosures that had been filled with lake water earlier that day.

Initial samples taken after dark revealed that exposure to chaoborids had rapidly (<4 h) stimulated a reappearance of reverse migrations in these previously non-migratory individuals (Fig. 2). Copepods descended to the bottom of all four predator enclosures and remained there until dawn. Not one copepod was detected in surface waters after dark, where added *Chaoborus* larvae were abundant. Copepods in controls (added lake water, no chaoborids) remained at shallow depths after dark, as did copepods in the *Chaoborus*-free lake (Fig. 1). Ascent on the following morning required their passing through the mass of descending *Chaoborus* larvae, indicating that reverse vertical migration had been re-adopted, and that the downward

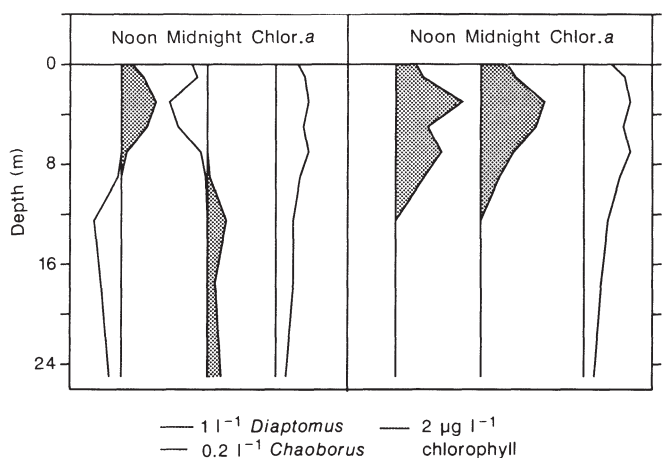


FIG. 1 Mean vertical distributions of the copepod *Diatomus kenai* (stippled) and the midge predator *Chaoborus trivittatus* (open) in Gwendoline Lake between 1100 and 1330 h (noon) and 2330 and 0200 h (midnight) on four dates during the month of July. Samples were taken by Clark-Bumpus sampler at 2-m depth intervals. Vertical distributions of chlorophyll *a* (pump samples at 0.5 m intervals) are for 5–50- μ m fraction collected during the day. Each figure is a mean of 12 samples (3 replicates on 4 dates) and is taken to represent the summer mean. Left-hand panel, vertical profiles 20 months before *Chaoborus* extermination by trout. Right-hand panel, vertical profiles 28 months after *Chaoborus* extermination.